

Nuclear transfer nTreg model reveals fate-determining TCR- β and novel peripheral nTreg precursors

Manching Ku^{a,1}, Shih-En Chang^a, Julio Hernandez^a, Justin R. Abadejos^a, Mohsen Sabouri-Ghomi^a, Niklas J. Muenchmeier^a, Anna Schwarz^a, Anna M. Valencia^a, and Oktay Kirak^{a,2}

^aDepartment of Immunology and Microbial Science, The Scripps Research Institute, La Jolla, CA 92037

Edited by Warren J. Leonard, National Heart, Lung and Blood Institute, Bethesda, MD, and approved March 8, 2016 (received for review December 3, 2015)

To study the development and function of “natural-arising” T regulatory (nTreg) cells, we developed a novel nTreg model on pure nonobese diabetic background using epigenetic reprogramming via somatic cell nuclear transfer. On RAG1-deficient background, we found that monoclonal FoxP3⁺ CD4⁺ Treg cells developed in the thymus in the absence of other T cells. Adoptive transfer experiments revealed that the thymic niche is not a limiting factor in nTreg development. In addition, we showed that the T-cell receptor (TCR) β -chain of our nTreg model was not only sufficient to bias T-cell development toward the CD4 lineage, but we also demonstrated that this TCR β -chain was able to provide stronger TCR signals. This TCR- β -driven mechanism would thus unify former per se contradicting hypotheses of TCR-dependent and -independent nTreg development. Strikingly, peripheral FoxP3⁺ CD4⁺ T cells expressing the same TCR as this somatic cell nuclear transfer nTreg model had a reduced capability to differentiate into Th1 cells but were poised to differentiate better into induced nTreg cells, both in vitro and in vivo, representing a novel peripheral precursor subset of nTreg cells to which we refer to as pre-nTreg cells.

somatic cell nuclear transfer | SCNT | nTreg | pre-nTreg | TCR- β

Natural arising regulatory T (nTreg) cells play a pivotal role in establishing and upholding peripheral tolerance (1, 2). FoxP3 had been identified as a key transcription factor not only important for the development of nTreg cells, but also for their function (3, 4). Loss-of-function mutations in the FoxP3 gene result in lack of Treg cells leading to widespread tissue inflammations (5, 6). The development and selection of nTreg cells in the thymus has been the subject of scientific debates for decades, and two contradicting hypotheses have been formulated. Although one hypothesis emphasized the development of nTreg cells in a T-cell receptor (TCR)-dependent manner, the other hypothesis postulated a TCR-independent mechanism. The TCR-dependent development is supported by the observation that TCR transgenic models generated from non-Treg cells did not possess any nTreg cells (7). In line with the TCR-dependent hypothesis is the notion that Treg cells developed in non-Treg TCR transgenic models only when the cognate antigen was expressed in the thymus (8–10). The TCR-independent hypothesis was proposed based on the observation that nTreg development was favored in a subset of CD4⁺ CD8[−] double-negative (DN) cells before the expression of a full TCR on the surface, and that development of Treg cells was less affected than that of conventional CD4⁺ T cells in pre-TCR- $\alpha^{-/-}$ (pT α) mice (11, 12). Given that the pT α , together with TCR- β , is expressed as pre-TCR at the CD4 CD8 DN stage 3 (DN3) before selection at the CD4 CD8 double-positive (DP) stage, a TCR-independent Treg development was indicated. In addition, although some studies investigating the TCR repertoire of conventional T cells (Tconv) and Treg cells demonstrated a partial overlap in support of the TCR-independent hypothesis, other studies reported no gross similarity of the TCR repertoire, in line with a TCR-dependent development (13–15).

TCR transgenic mice have been valuable tools in better understanding the role of T cells in health and disease. Several

mouse models had been made to study the development and function of nTreg cells. First studies used existing non-Treg TCR transgenic mice and expressed the cognate antigen in the thymus (10). This approach demonstrated that an nTreg-like phenotype could be induced in the thymus. Other studies generated Treg TCR transgenic models by isolating TCRs from Treg cells or by using a fixed TCR β -chain approach (16–18). Surprisingly, none of these Treg TCR transgenic models possessed any major nTreg population (less than 0.1% of CD4⁺ T cells) in the thymus when crossed onto a Rag-deficient background. This result had led to the hypothesis that intraclonal competition might inhibit nTreg development in a monoclonal setting, and was supported by the observation that thymic Treg cells were found when bone marrow from TCR-transgenic and WT were mixed and injected into lethally irradiated recipient mice.

We recently showed that epigenetic reprogramming through somatic cell nuclear transfer (SCNT) can be used to develop novel T- and B-cell mouse models (19, 20). We hypothesized that in SCNT mice, the more physiological TCR expression from the endogenous TCR locus under the control of the endogenous promoter and enhancer regions might facilitate better nTreg development. Although our initial SCNT models were based on the hybrid strain C57BL/6 \times BALB/c F1 (B6CF1), we reasoned that such F1-based SCNT models are not suitable for immunological studies. Hence, to avoid well-known artifacts from hybrid strains, we developed a novel SCNT Treg model on pure nonobese

Significance

T cells generate their T-cell receptors (TCR) through somatic rearrangement of their underlying genomic V(D)J regions. Contrary to previous transgenic TCR models, our TCR models generated through somatic cell nuclear transfer are precise copies of the original T cell. Here, we developed a novel somatic cell nuclear transfer model of natural arising regulatory T (nTreg) cells. In our monoclonal model, we found a well-defined nTreg population in the thymus, contradicting previous reports that intraclonal competition and thymic niche are limiting factors in nTreg development. Moreover, we found a novel fate-determining role for the TCR β -chain in nTreg cells. Interestingly, we also discovered a novel T-cell subset that functions as peripheral precursor of nTreg cells.

Author contributions: M.K., S.-E.C., J.H., J.R.A., M.S.-G., N.J.M., A.S., A.M.V., and O.K. designed research; M.K., S.-E.C., J.H., J.R.A., M.S.-G., N.J.M., A.S., A.M.V., and O.K. performed research; M.K. and O.K. contributed new reagents/analytic tools; M.K., S.-E.C., J.H., J.R.A., M.S.-G., N.J.M., A.S., A.M.V., and O.K. analyzed data; and M.K. and O.K. wrote the paper.

The authors declare no conflict of interest.

This article is a PNAS Direct Submission.

Data deposition: The data reported in this paper have been deposited in the Gene Expression Omnibus (GEO) database, www.ncbi.nlm.nih.gov/geo (accession no. GSE70156).

¹Present address: Salk Institute for Biological Studies, La Jolla, CA 92037.

²To whom correspondence should be addressed. Email: kirak@scripps.edu.

This article contains supporting information online at www.pnas.org/lookup/suppl/doi:10.1073/pnas.1523664113/-DCSupplemental.

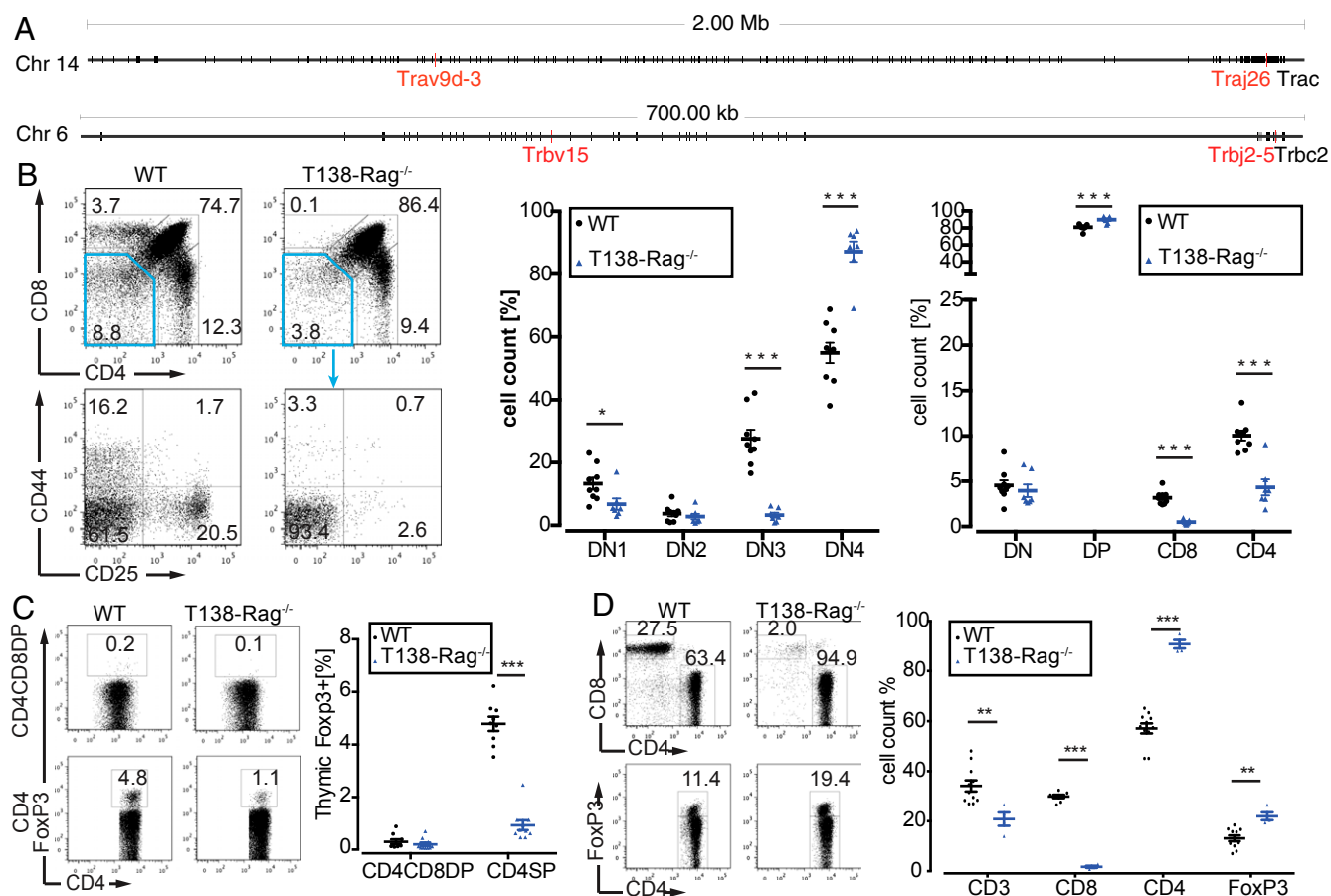


Fig. 1. Generation of a novel SCNT-derived nTreg model. (A) Identification of the V(D)J rearrangements for TCR- α (Upper) and TCR- β (Lower) chains in the SCNT mouse model using useast.ensembl.org/index.html. The β D2 segment of the TCR- β is not shown because of space limitation. (B) Representative flow cytometric analysis of T-cell development in the thymus of WT and T138 (Left). Scatter plots display various T-cell subpopulations of WT (black circles), and T138-Rag^{-/-} (blue triangles) mice. (C) Representative flow cytometric analysis of FoxP3⁺ cells in CD4 CD8 DP T cells (Upper) and CD4 single-positive (SP) T cells (Lower) in WT (Left) and T138 (Right) mice. Scatter plot (Right) shows all data points. (D) Statistical analysis of various lymphocyte populations in spleen. Each symbol represents an individual mouse. Error bars are expressed as mean \pm SEM; * P < 0.05, ** P < 0.01, *** P < 0.001.

diabetic (NOD) background to study the development and function of nTreg cells.

Results

Generation of a Novel SCNT-Derived nTreg Model. We had previously shown that inhibitors of histone deacetylases could improve SCNT of donor cells from pure BALB/c background (20). Here, we applied the SCNT approach to donor Treg cells from pure NOD background. To use an unbiased approach, we used NOD-FoxP3^{GFP}-Rag^{+/-} mice in which the TCR- α and - β locus were in WT configuration. FoxP3⁺ CD4⁺ Treg cells were sorted from the spleen of healthy NOD-FoxP3^{GFP}-Rag^{+/-} mice using flow cytometry, and used as donor cells for SCNT. Embryonic stem cells were derived from resulting SCNT blastocysts, and used to generate chimeric mice, as described previously (19, 20). A single cross of these chimeric mice with NOD-Rag^{-/-} resulted in NOD-TCR $\alpha\beta$ -FoxP3^{GFP}-Rag^{-/-} mice, which can be directly analyzed. We refer to this SCNT Treg line as T138. We first identified the VJ rearrangement underlying the TCR- α as V9d-3-J26 combination (Fig. 1A, Upper), and the V(D)J rearrangement of the TCR- β as V15-D2-J2-5 (Fig. 1A, Lower). To determine whether this SCNT model might represent an nTreg cell, we focused our initial analysis on T138-Rag^{-/-} mice. We found well-defined FoxP3⁺ CD4⁺ Treg cells in the thymus of our SCNT-derived model when crossed onto a Rag-deficient background. This result clearly demonstrated that a monoclonal CD4⁺ T-cell population

could indeed give rise to nTreg cells when the physiological TCR is expressed from the physiological locus under the control of the endogenous promoter and enhancer regions (Fig. 1B and C). We determined that the percentage of thymic FoxP3⁺ CD4⁺ T cells was about 1.5% of the CD4⁺ T cells in monoclonal T138-Rag^{-/-} mice. For comparison, polyclonal WT NOD mice possessed about 5% FoxP3⁺ CD4⁺ T cells. Interestingly, although in the spleen the percentage of FoxP3⁺ CD4⁺ T cells in T138-Rag^{-/-} was higher than in WT NOD mice (about 22% in T138 compared with about 12% in WT) (Fig. 1D), we found a relative decrease in mesenteric lymph nodes (about 5% in T138 versus about 9% in WT) (Fig. S1; see Fig. S2 for absolute numbers).

Thymic T-Cell Development After Adoptive Transfer. Previous transgenic Treg models had virtually no Treg cell development in the thymus when maintained on Rag-deficient background (16–18). However, after adoptive transfer of bone marrow into irradiated recipient mice, an increase in thymic Treg cells was observed. In addition, the number of Treg cells in the thymus increased when fewer bone marrow cells were transferred. This finding has led to the conclusion that intraclonal competition might hamper Treg development (21). As shown in Fig. 1, our SCNT-derived T138 had a well-defined thymic Treg cell population on Rag-deficient background, thus demonstrating that nTreg cells can develop in a monoclonal setting. However, to test whether there is an inverse correlation between the number of transferred bone marrow cells

and the number of developing Treg cells in the thymus, we performed a competitive adoptive transfer experiment by transferring bone marrow from T138-Rag^{-/-} (CD90.2) and WT NOD competitors (CD90.1) into irradiated NOD hosts (CD90.1-CD90.2 DP). We performed flow cytometric analysis of recipient mice 7 wk after adoptive transfer, and found that the percentage of FoxP3⁺ CD4⁺ T cells from T138 was increasing with a decreasing amount of transferred bone marrow cells (Fig. 2*A* and Fig. S3). Given the variability in engraftment, we analyzed the development of thymic FoxP3⁺ CD4⁺ T cells relative to the contribution of T138 to the host. As shown in Fig. 2*B, Left*, we found an inverse correlation ($R^2 = -0.785$) between Treg cell development and bone marrow contribution as had been reported previously (16–18). A comparison between the absolute numbers of FoxP3⁺ T cells in the thymic CD4SP population revealed that even though the frequencies of FoxP3⁺ T cells among the CD4SP cells increased, the absolute numbers never reached those found in T138-Rag1^{-/-} mice (Fig. 2*B, Right*, blue dotted line, and Fig. S24).

Cell Fate-Determining TCR- β in nTreg Cells. During our initial breeding between T138 (NOD-TCR $\alpha\beta$ -FoxP3^{GFP}-Rag^{+/-}) and NOD-Rag1^{-/-} or NOD-FoxP3^{GFP}, we routinely analyzed the spleen from these offspring. During this screen we found a relative increase in CD4⁺ T cells in about 50% of the offspring. This was surprising because an increase in CD4⁺ T cells in a CD4⁺ TCR model is only observed when both the TCR α -chain and TCR β -chain are present, which holds true for both traditional transgenic and SCNT-derived T-cell models. An increase in CD4⁺ T cells should only be seen in 25% of the offspring. Further analysis revealed that expression of the TCR β -chain alone with a WT TCR- α locus was sufficient to bias T cells away from the CD8⁺ lineage and toward the CD4⁺ lineage in the spleen

(Fig. 3*A*) and lymph node (Fig. S44), whereas the fraction of FoxP3⁺ CD4⁺ T cells remained comparable to WT mice. To determine whether this bias can already be seen during development, we analyzed the thymus of T138 β mice using flow cytometry. As shown in Fig. 3*B*, a bias in T-cell development away from the CD8⁺ lineage can already be found in the thymus. Given that we had identified TRBV15 (also referred to as V β 12) as part of the TCR β -chain in T138, we analyzed the extent to which this TCR β -chain can bias T-cell development (Fig. S4C). We found that the majority (over 80%) of T cells developed into CD4⁺ T cells in mice expressing the T138-derived TCR β -chain. Interestingly, we also found a small fraction (about 10%) of CD8⁺ T cells that were able to develop by using the T138-derived TCR β -chain. Given that mice carrying one allele of the T138-derived TCR β -chain possessed about 2% of CD4⁺ and 2% CD8⁺ T cells that did not use the T138-derived TCR β -chain, we crossed this TCR β -chain to homozygosity for future experiments, resulting in T138- $\beta\beta$. To determine whether TCR-levels are increased in T138- $\beta\beta$, we performed flow cytometric analysis. As shown in Fig. S4D, FoxP3⁺ CD4⁺ T cells from WT, T138 and T138- $\beta\beta$ mice expressed similar levels of TCR- β . Interestingly, although FoxP3⁺ CD4⁺ T-cell from WT and T138- $\beta\beta$ expressed similar levels of TCR- β , T138 had a higher mean fluorescence intensity because of the lack of T cells that expressed low levels of TCR- β (red solid line).

Characterization of FoxP3⁺ CD4⁺ T Cells in T138. Given that we found conventional-like FoxP3⁺ CD4⁺ T cells in thymus, spleen, and lymph nodes expressing the same TCR as an nTreg cell, we investigated whether these FoxP3⁺ CD4⁺ T cells were anergic or whether it might be possible to activate and differentiate these cells in vitro. FoxP3⁺ CD4⁺ T cells were isolated from the spleen of T138-FoxP3^{GFP}-Rag^{-/-} mice and compared with WT NOD-FoxP3^{GFP} mice. Although it was indeed possible to differentiate FoxP3⁺ CD4⁺ T cells from T138 into Th1 cells, the overall efficiency was significantly lower than that of FoxP3⁺ CD4⁺ T cells from WT-derived T cells (about 21% for T138 versus 52% for WT) (Fig. 4*A*). Given that we had observed a skewing of T-cell development toward the CD4 lineage in mice expressing the T138-derived TCR β -chain, we determined their ability to differentiate into Th1 cells. As shown in Fig. 4*A*, FoxP3⁺ CD4⁺ T cells from T138 β mice differentiated into Th1 cells with similar efficiencies as WT cells. Of note, to ensure use of T138 β , we analyzed mice homozygous for the rearranged TCR- β (T138- $\beta\beta$). When we cultured FoxP3⁺ CD4⁺ T cells under conditions that favored Treg differentiation, we found that the majority of FoxP3⁺ CD4⁺ T cells from T138 differentiated into Treg cells, with a significantly higher efficiency than both WT NOD control T cells and T cells expressing T138-derived TCR β -chain (71% for T138 vs. 46% for WT and 47% for T138- $\beta\beta$) (Fig. 4*B*). As mentioned above, we found a small portion of T cells (about 10%) that developed into CD8⁺ T cells in mice expressing the T138-derived TCR β -chain. To determine whether their plasticity is impacted, we cultured these CD8⁺ T cells under condition that favor IFN- γ or FoxP3-expression. Strikingly, we found that CD8⁺ T cells expressing the T138-derived TCR β -chain had a significantly reduced capability to up-regulate FoxP3 (about 5% for CD8⁺ T138- $\beta\beta$ compared with about 26% for WT CD8⁺ T cells) (Fig. 4*C*), whereas their ability to up-regulate IFN- γ was comparable to WT CD8⁺ T cells (Fig. S54). Given this surprising bias in T-cell differentiation during in vitro differentiation, we performed adoptive transfer experiments to determine their differentiation during homeostatic proliferation. As shown in Fig. 4*D*, FoxP3⁺ CD4⁺ T cells from T138-Rag^{-/-} mice differentiated into FoxP3⁺ Treg cells significantly better than WT FoxP3⁺ CD4⁺ T cells when adoptively transferred into NOD-Rag^{-/-} mice.

It had been reported that recent thymic emigrants (RTE) are enriched in cells that can differentiate better into FoxP3⁺ CD4⁺

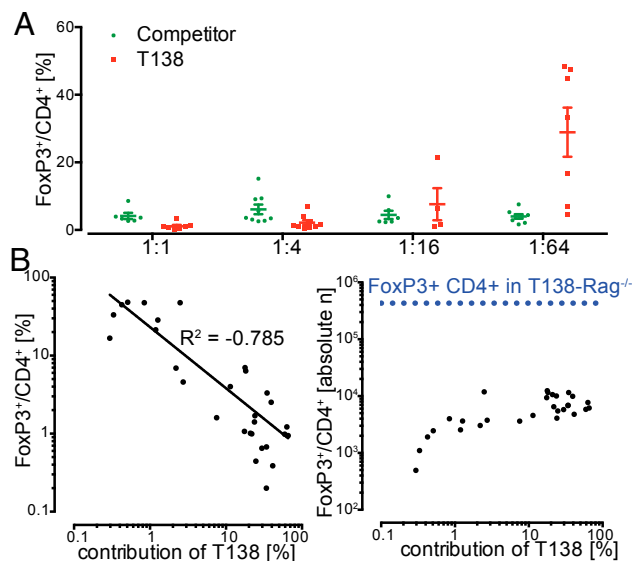


Fig. 2. Thymic T-cell development after adoptive transfer. (*A*) The progenitor and stem cell population was enriched from the bone marrow of WT (CD90.1, green) and T138-Rag^{-/-} (CD90.2, red) mice, mixed at indicated ratios, and injected into irradiated NOD hosts (CD90.1 CD90.2 DP). Flow cytometry analysis of thymus was performed 7 wk after adoptive transfer. Scatter plot summarizing the percentages of Treg cell in thymic CD4 SP subsets from WT (green circle) and T138 (red squares) donors at different ratios. Each symbol represents an individual mouse. Error bars are expressed as mean \pm SEM. (*B*) The data are the same as shown in *A*. The frequency (*Left*) or absolute numbers (*Right*) of FoxP3⁺ T cells developed from T138-derived bone marrow is plotted against the contribution of T138 to the recipient mice. Blue dashed line indicates absolute numbers of FoxP3⁺ T cells in the thymic CD4SP population in T138-Rag^{-/-} mice.

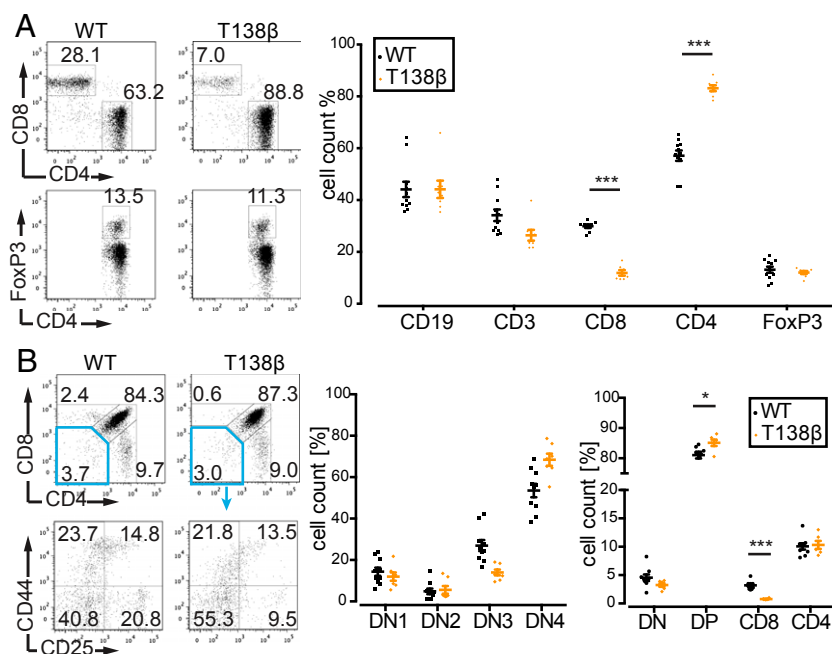


Fig. 3. Cell fate-determining TCR- β in nTreg cells. (A) Flow cytometric analysis of T cells in the spleen of WT NOD (black circles), and T138 β (yellow squares) mice. Representative plots are shown on (Left) and a scatter plot (Right). (B) Flow cytometric analysis of thymic development of WT (black circles), and T138 β (yellow squares) mice. Representative plots are shown (Left) and a scatter plot (Right). Each symbol represents an individual mouse. Error bars are expressed as mean \pm SEM; * P < 0.05, *** P < 0.001.

T cells (22). To determine whether the bias toward FoxP3 expression in FoxP3 $^{-}$ CD4 $^{+}$ T cells in our T138 model is because of an enlarged RTE population, we performed flow cytometric analysis of thymus and spleen. As shown in Fig. S5 B and C, we found no increase in RTE in the spleen of T138 (mean values: 2.77% in WT, 1.36% in T138-Rag $^{-/-}$, and 2.41% in T138- β). This finding indicated to us that the peripheral FoxP3 $^{-}$ CD4 $^{+}$ T cells expressing the same TCR as the nTreg model are not conventional CD4 $^{+}$ T cells, but rather a precursor population that is poised away from Th1 and toward Treg cells. Herein, we refer to this novel T-cell subset as “pre-nTreg” cells.

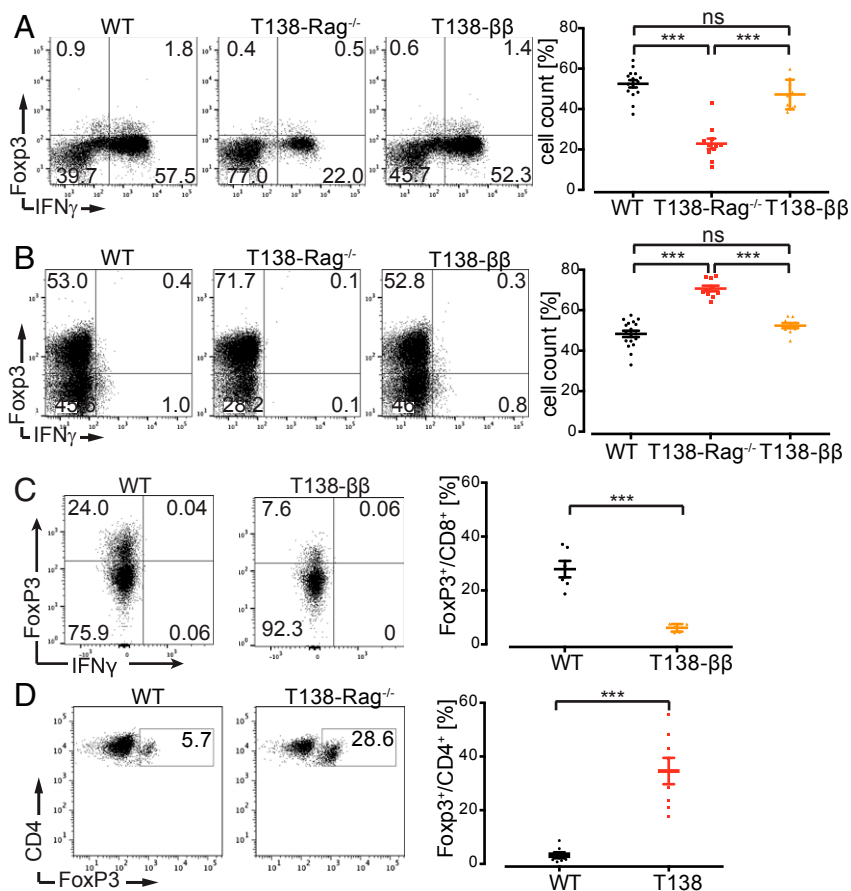
TCR Strength in Pre-nTreg and nTreg Cells. Many reports pointed toward an interaction between the TCR and its peptide-MHC complex that might be of higher affinity in nTreg cells than the average conventional CD4 $^{+}$ T cells (9, 23–26). Given that our nTreg-derived TCR β -chain was capable of skewing thymic development toward the CD4 lineage, as well as T-cell differentiation, we wanted to determine whether this TCR β -chain might be able to provide stronger TCR signal than WT CD4 $^{+}$ T cells. It had been shown that Nur77 levels correlate directly with TCR strength and are independent of any inflammatory stimuli (26). Thus, we used endogenous Nur77 levels to determine the TCR strength in our FoxP3 $^{+}$ nTreg and FoxP3 $^{-}$ pre-nTreg cells, as well as in FoxP3 $^{-}$ and FoxP3 $^{+}$ CD4 $^{+}$ T cells expressing the T138-derived TCR β -chain. As shown in Fig. 5, although the FoxP3 $^{+}$ population of CD4 $^{+}$ T cells expressing WT TCR or T138-derived TCR β -chain maintained significantly higher Nur77 levels than their FoxP3 $^{-}$ counterparts, we observed no significant difference between FoxP3 $^{-}$ pre-nTreg and FoxP3 $^{+}$ nTreg cells from T138 mice. FoxP3 $^{-}$ CD4 $^{+}$ T cells expressing T138-derived TCR β -chain showed higher Nur77 levels than FoxP3 $^{-}$ CD4 $^{+}$ T cells from WT and T138 mice. Surprisingly, FoxP3 $^{+}$ CD4 $^{+}$ nTreg cells had significant lower Nur77 levels than polyclonal FoxP3 $^{+}$ CD4 $^{+}$ T cells from WT mice, and FoxP3 $^{+}$ CD4 $^{+}$ T cells expressing T138-derived TCR β -chain. Given our surprising finding that CD4 $^{+}$ FoxP3 $^{-}$ pre-nTreg and CD4 $^{+}$ FoxP3 $^{+}$ nTreg had similar

Nur77 levels, we decided to determine the levels of CD5. CD5 can function as a negative regulator of TCR signaling, and its expression level is directly correlated to the TCR strength (27, 28). As shown in Fig. 5B, the CD5-levels of FoxP3 $^{+}$ and FoxP3 $^{-}$ CD4 $^{+}$ T cells in T138 are almost identical, thus confirming our Nur77 data.

DNA Methylation and FoxP3 Expression in Pre-nTreg and nTreg Cells.

The presence of FoxP3 $^{+}$ CD4 $^{+}$ T cells on Rag-deficient background indicated that our SCNT-derived model represented nTreg cells. However, to further validate that our novel mouse model resembles nTreg cells, we performed DNA CpG-methylation analysis. The conserved noncoding sequence 2 in intron 1 of *FoxP3* is also known as Treg-specific demethylation region and has been shown to be hypomethylated in Treg cells (29–31). A few additional loci have been suggested to play important roles in Treg cells, including *Il2ra* and *Ctla4* (32). To determine the methylation status of these “Treg representative regions,” we first focused on the *FoxP3* locus in thymic CD4 $^{+}$ CD8 $^{+}$ DP cells, and splenic FoxP3 $^{+}$ CD4 $^{+}$ T cells. As shown in Fig. 6A, we found that the *FoxP3* intron 1 in T138 and WT NOD mice was methylated in CD4 $^{+}$ CD8 $^{+}$ DP cells, and completely demethylated in splenic FoxP3 $^{+}$ CD4 $^{+}$ T cells. We also found that although the *FoxP3* locus upstream –1,500 bp (FoxP3 –1500) in T138 underwent more CpG demethylation compared with WT (Fig. 6B, Lower), the *Il2ra* intron 1a and *Ctla4* exon 2 loci showed hypomethylated CpG in T138 at levels comparable to WT (Fig. 6C and D). Surprisingly, when we determined the methylation status of the same loci in splenic FoxP3 $^{-}$ CD4 $^{+}$ pre-nTreg cells, we found the *FoxP3* intron 1 locus as well as the other examined loci with methylation levels comparable to WT FoxP3 $^{-}$ CD4 $^{+}$ T cells (Fig. 6E–H).

To determine whether *FoxP3* expression induced after in vitro differentiation was maintained stable, we differentiated FoxP3 $^{-}$ CD4 $^{+}$ T cells from WT NOD, T138-Rag $^{-/-}$, and mice expressing the T138-derived TCR β -chain. After 4 d of in vitro differentiation under FoxP3-inducing conditions, FoxP3 GFP -expressing



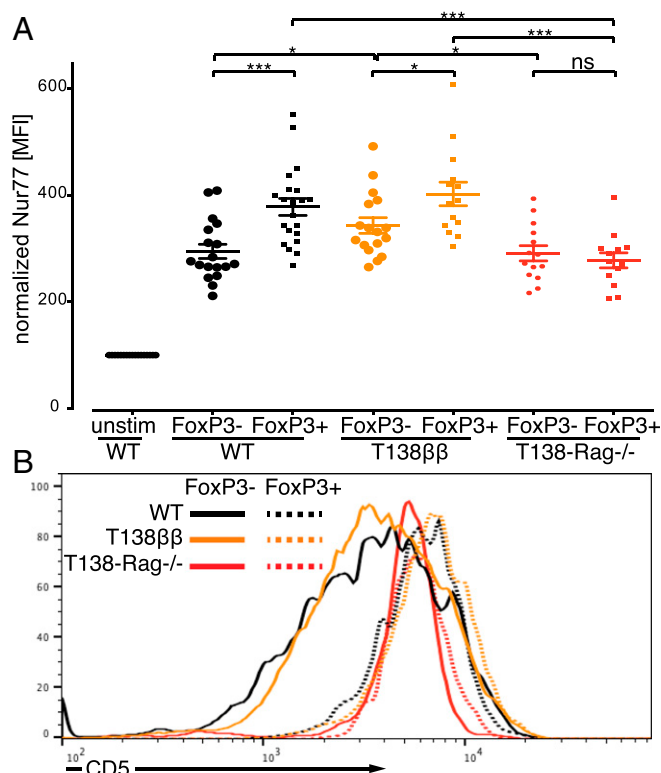


Fig. 5. TCR strength in pre-nTreg and nTreg cells. (A) Using endogenous Nur77 levels, the TCR strength of FoxP3⁻ and FoxP3⁺ CD4⁺ T cells from T138-Rag^{-/-} (red symbols) mice was determined. We also analyzed Nur77 levels in FoxP3⁻ and FoxP3⁺ CD4⁺ T cells expressing the nTreg-derived TCR β-chain paired with polyclonal TCR α-chains (T138-β; orange symbols). FoxP3⁻ and FoxP3⁺ CD4⁺ T cells from NOD mice served as controls (black symbols). Nur77 levels were normalized to unstimulated CD4⁺ T cells (open circles). (B) CD5 levels were determined in FoxP3⁻ and FoxP3⁺ CD4⁺ T cells from WT, T138-Rag^{-/-}, and T138-β. The experiment was performed as two independent duplicates. Representative plots are shown. Error bars are expressed as mean ± SEM; **P* < 0.05; ***P* < 0.01; ****P* < 0.001.

FoxP3⁻ CD4⁺ pre-nTreg cells were most different from the other three populations (Fig. 7A). Strikingly, FoxP3⁻ CD4⁺ pre-nTreg cells were most different from polyclonal FoxP3⁻ CD4⁺ T cells of WT mice. To better visualize differentially expressed genes among all four cell populations, we generated fold-change/fold-change (FC/FC) scatter plots (Fig. 7B). The ratio of (FoxP3⁺ T138 FC) versus (FoxP3⁻ T138 FC) was plotted against the ratio of (FoxP3⁺ WT FC) versus (FoxP3⁻ WT FC). In this comparison, genes that are up-regulated in both nTreg and polyclonal FoxP3⁺ CD4⁺ Treg cells from WT are found in the upper right quadrant. This group contained several genes known to be expressed in Treg cells, such as FoxP3, CD25, Ctla4, Ikzf2 (Helios), and Ikzf4 (Eos) (33–35). In Fig. S7A, the ratio of (FoxP3⁺ T138 FC) versus (FoxP3⁺ WT FC) was plotted against the ratio of (FoxP3⁻ T138 FC) versus (FoxP3⁻ WT FC). In this comparison, genes that are up-regulated in both nTreg and pre-nTreg cells are found in the upper right quadrant. We performed network analysis to determine whether the FoxP3 network in T138 differed from polyclonal FoxP3⁺ CD4⁺ Treg cells from WT mice. As shown in Fig. S7B and C, the FoxP3 network in monoclonal nTreg cells differed greatly from polyclonal FoxP3⁺ CD4⁺ Treg cells, suggesting that the transcription factor FoxP3 and its cofactors may cooperate in a more concerted effort in executing nTreg functions compared with heterogeneous polyclonal Treg cells in WT mice. We also performed transcription factor target analysis to determine genes that contained FoxP3

binding motif in their promoter region and that were differentially expressed between monoclonal nTreg cells and polyclonal FoxP3⁺ CD4⁺ Treg cells. We found 33 genes with the FoxP3 binding motif that were significantly up-regulated in nTreg cells, such as *ErbB2*, *Rora*, and *Fos*, and 26 genes that were up-regulated in polyclonal FoxP3⁺ CD4⁺ Treg cells, including *Bach2*, *Ikzf4* (Eos), and *Rorc* (Fig. S8). In addition, the transcription factor nuclear-factor of activated T cells (Nfat) has been shown to play an important role in Treg cells (36–38). We found 79 genes with an Nfat binding motif that were significantly up-regulated in nTreg cells, including *Il7r*, *Meis1*, and *Gata3*, and 52 genes that were up-regulated in polyclonal FoxP3⁺ CD4⁺ Treg cells, including *Nr4a3*, *Il6st*, and *Tiam1* (Fig. S9).

Discussion

To better understand the development and function of CD4⁺ nTreg cells, we developed a novel model using FoxP3⁺ CD4⁺ T cells from the spleen of NOD mice as donor cells for SCNT. We reasoned that in this novel SCNT model, both the pure background and the expression of the TCR from its physiological locus should facilitate nTreg development. Indeed, our data revealed that thymic FoxP3⁺ CD4⁺ nTreg cells did develop in the thymus of SCNT-derived mice on Rag-deficient background demonstrating that monoclonal nTreg cells did not require other polyclonal T cells for their development, as previously hypothesized (16–18). Our competitive bone marrow transfer experiment confirmed previous data showing an inverse correlation between the contribution and relative frequency of Treg cells. However, a closer look at the absolute numbers showed that the amount of FoxP3⁺ CD4⁺ T cells in the thymic CD4SP population never reached those found in T138-Rag^{-/-} mice (Fig. 2B, blue dotted line). This result demonstrated that the niche is not the limiting factor in nTreg development. This finding is in contrast to previously published data, in which the absolute number of FoxP3⁺ T cells in the thymic CD4SP population after bone marrow transfer surpassed the absolute number in the parental TCR transgenic line (16).

Strikingly, the TCR β-chain in our nTreg model had several unique features: (i) when paired with an nTreg-derived TCR α-chain it gave rise to FoxP3⁺ nTreg cells and FoxP3⁻ pre-nTreg cells; (ii) when paired with polyclonal TCR α-chains, T-cell development was skewed toward the CD4 lineage, but without any bias in T-cell differentiation toward Th1 or Treg in CD4⁺ T cells; and (iii) when paired with polyclonal TCR α-chains giving rise to CD8⁺ T cells, their differentiation was skewed away from FoxP3-expression. Our results point toward a novel interaction between nTreg-derived TCR β-chain and p-MHC-II, as well as p-MHC-I that has so far been disregarded. In addition, we were also able to demonstrate that an nTreg-derived TCR β-chain can provide stronger TCR signals. To our knowledge, this is the first report of any TCR β-chain with such a major impact on T-cell development, T-cell differentiation, and TCR strength. Given that the TCR β-chain rearranges first and is presented on the surface at the DN3 stage, we propose herein a model in which nTreg development is initially determined by TCR β-chains in a first step (Fig. 8). This TCR-β-deterministic model would unify the two current per se contradictory hypotheses of TCR-dependent and -independent nTreg development (7–15). We hypothesize that as part of the TCR complex, some unique TCR β-chains are able to direct development toward the CD4 lineage in a first step, requiring an nTreg-permissive TCR α-chain in a second step to fully commit to either pre-nTreg or nTreg cells. This TCR β-deterministic model is further supported by data demonstrating that Treg development was negatively impacted in a TCR transgenic mouse model expressing a TCR β-chain from a CD8⁺ T-cell (39). We hypothesize that a unique interaction between TCR β-chains and p-MHC-II might provide sufficient signal to drive nTreg development, which would explain why their development is less impacted in preTCR-α^{-/-}

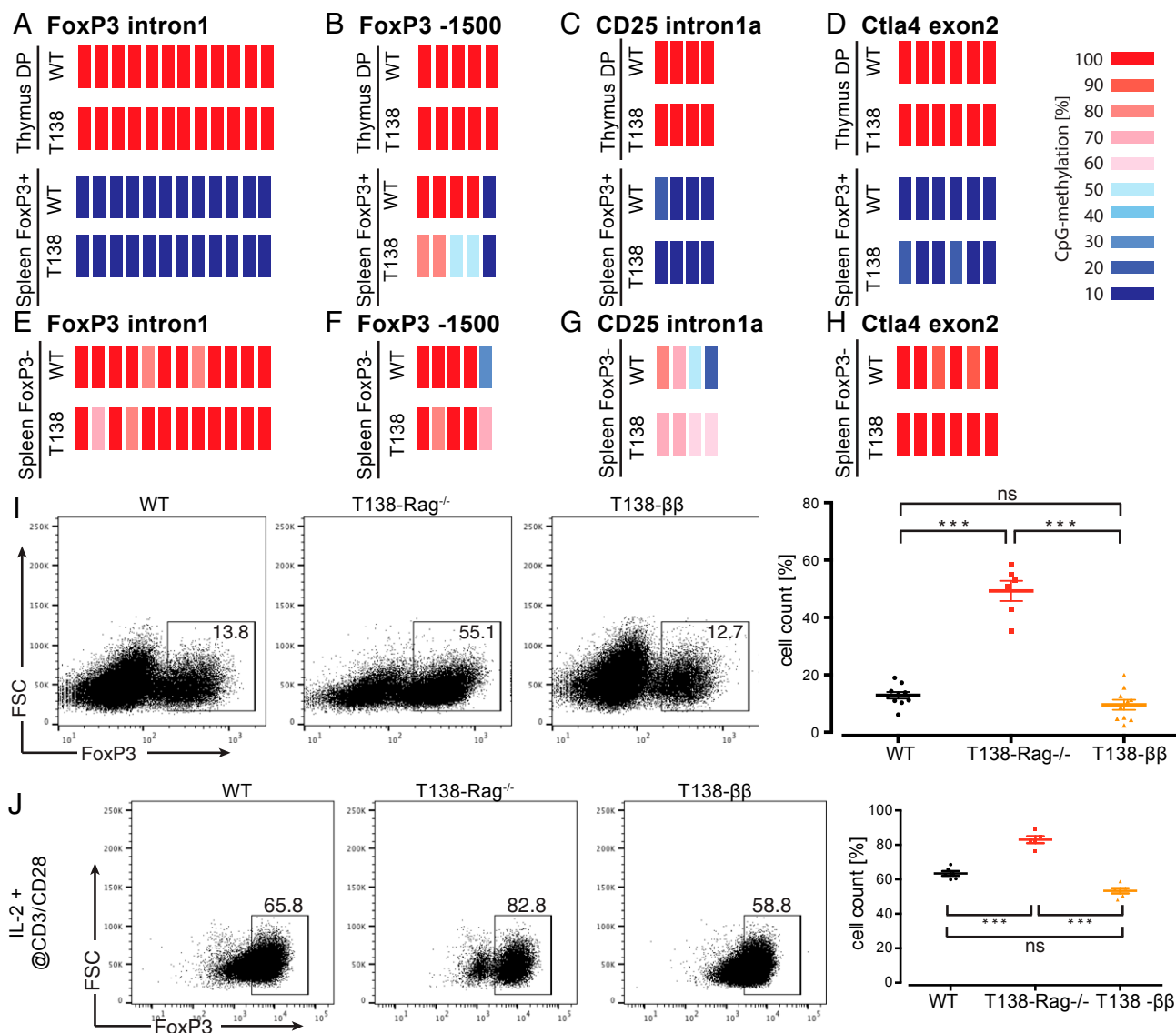


Fig. 6. DNA methylation analysis and stability of FoxP3 expression. Using bisulfite sequencing, the CpG methylation status of FoxP3 intron 1 (also known as Treg-specific demethylation region) (A), FoxP3 –1500 (B), CD25 intron 1a (C), and CTLA4 exon 2 (D) was determined in nTreg mice and compared with WT mice. The methylation status of FoxP3 intron 1 (A) and FoxP3 –1500 (B) was determined in thymic CD4⁺CD8⁺ DP cells (Upper) and splenic FoxP3⁺ CD4⁺ T cells (Lower). We also determined the methylation status of FoxP3 intron 1 (E), FoxP3 –1500 (F), CD25 intron 1a (G), and CTLA4 exon 2 (H) in splenic FoxP3⁺ CD4⁺ T cells from T138 and WT mice. (I) To determine the stability of FoxP3 expression, splenic FoxP3⁺ CD4⁺ T cells from NOD-Foxp3^{GFP} (WT), T138-Foxp3^{GFP}-Rag^{-/-}, or T138-ββ-Foxp3^{GFP} mice were sorted using flow cytometry. After 4 d of in vitro culture in the presence of TGF-β to induce FoxP3-expression, FoxP3^{GFP}-expressing cells were sorted using flow cytometry and cultured for an additional 5 d in the absence of TGF-β to determine stability of FoxP3 expression. (J) To determine the stability of FoxP3-expression in FoxP3⁺ CD4⁺ T cells, FoxP3^{GFP}-expressing cells purified and cultured under indicated conditions for 4 d. Error bars are expressed as mean ± SEM; ****P* < 0.001.

mice, and why preferential nTreg development can be observed in a subpopulation of developing T cells at the DN stage, hence a seemingly TCR-independent development (11). The existence of unique TCR β-chains that support nTreg development, would thus also explain why most TCR-transgenic mouse models do not contain any nTreg cells, and hence argue for a TCR-dependent development.

Using a Nur77-GFP reporter mouse, it had been shown that Treg cells possess higher TCR strength than conventional CD4⁺ T cells (26). It is commonly believed that this is a result of a higher affinity for self-peptides referred to as agonist. However, in light of our new data demonstrating that nTreg-derived TCR β-chain can provide stronger TCR signal, and in line with our data demonstrating no significant difference in TCR strength

between FoxP3⁺ pre-nTreg and FoxP3⁺ nTreg cells, we hypothesize that recognition of agonists might play a less dominant role in nTreg development than previously hypothesized. This observation is further supported by our data, demonstrating that there is also no difference in CD5-levels between the FoxP3⁺ and FoxP3⁺ CD4⁺ population in our T138 model. Given that no physiological agonists of nTreg cells have been identified so far, more studies are needed to determine the role of nTreg TCR β- and α-chains, and their interaction with peptide-MHC in nTreg development.

As shown, our SCNT-derived nTreg model contained FoxP3⁺ CD4⁺ T cells in the thymus, spleen, and lymph nodes when maintained on Rag-deficient background. These FoxP3⁺ CD4⁺ T cells expressed the same TCR as nTreg cells. Differentiation

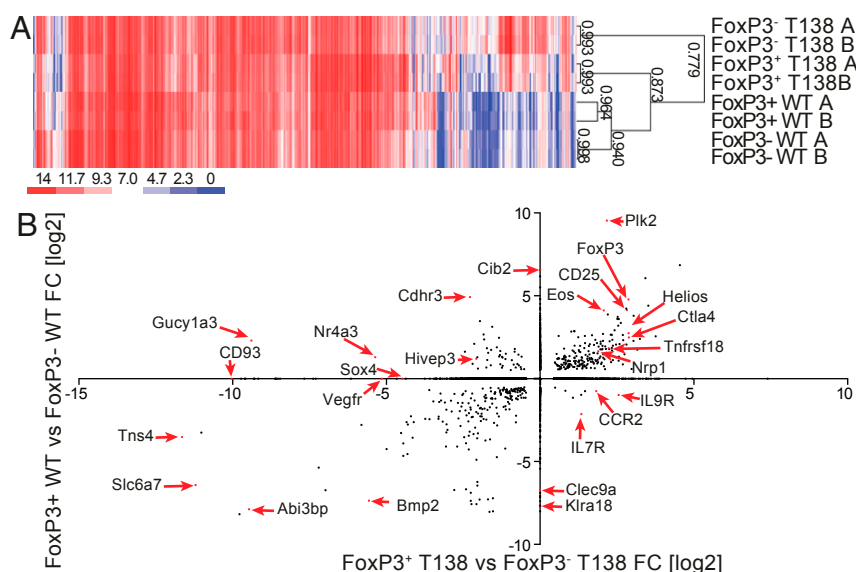


Fig. 7. Transcriptome profiling of pre-nTreg and nTreg cells. (A) FoxP3⁺ and FoxP3⁻ CD4⁺ were sorted from NOD-Foxp3^{GFP} (WT) or T138-Foxp3^{GFP}-Rag^{-/-} mice using flow cytometry, and used for RNA-Sequencing. RNA-Seq data were analyzed using genome-wide hierarchical clustering. (B) The FC of differentially expressed genes in FoxP3⁺ CD4⁺ T138 versus FoxP3⁻ CD4⁺ T138, were plotted against the FC of differentially expressed genes in FoxP3⁺ CD4⁺ T cells versus FoxP3⁻ CD4⁺ T cells from WT mice.

experiments showed that these FoxP3⁻ CD4⁺ T cells could differentiate at high efficiency into FoxP3⁺ CD4⁺ T cells, whereas their differentiation into Th1 cells was significantly less efficient compared with CD4⁺ T cells from WT or T138-ββ mice (Fig. 4). Strikingly, when FoxP3⁻ CD4⁺ T cells were adoptively transferred into Rag-deficient mice, these cells readily differentiated into

FoxP3⁺ CD4⁺ T cells. In addition, once FoxP3-expression was induced in pre-nTreg cells in the presence of TGF-β, it was maintained and expressed in the majority of cells in the absence of TGF-β, contrary to FoxP3-induced cells from WT and T138-ββ mice (Fig. 6I). Surprisingly, this more stable expression of FoxP3 was not a result of demethylation of the Treg-specific demethylation

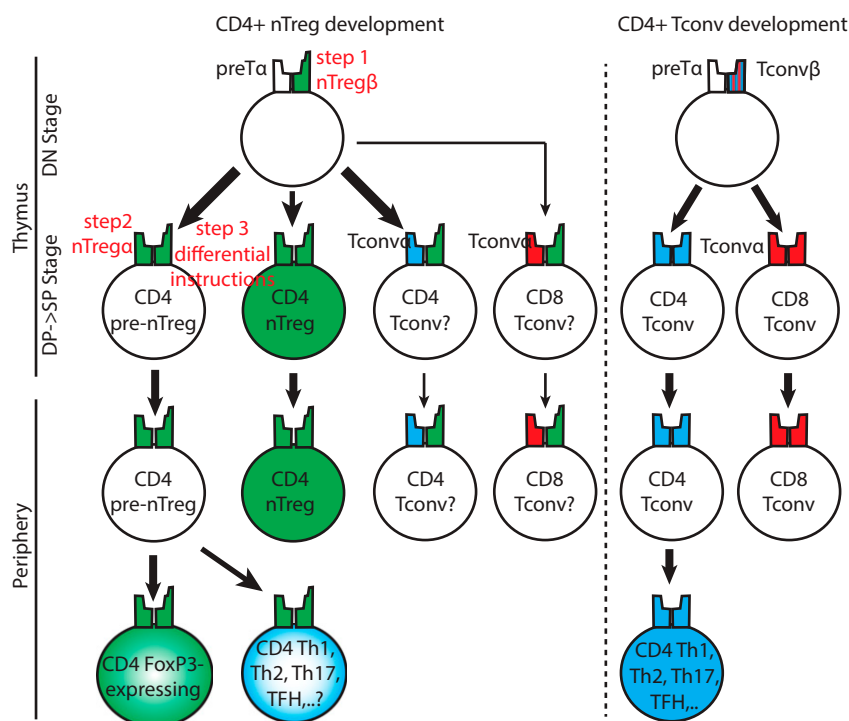


Fig. 8. Model of nTreg development. In a first step, a unique V(D)J rearrangement at the TCR-β locus (green polygon) poises T-cell development toward the CD4 lineage. In a second step, expression of TCR-α (green polygon) that supports nTreg development leads to the development of FoxP3⁻ CD4⁺ pre-nTreg and FoxP3⁺ CD4⁺ nTreg cells (green filled), likely due to differential instructions (step 3). Peripheral induction of CD4⁺ pre-nTreg cells leads to FoxP3-expressing CD4⁺ T cells (green gradient).

region (Fig. S64). We were also able to show that FoxP3⁺ CD4⁺ nTreg cells in T138 maintained a more stable FoxP3-expression in the absence of TGF- β than FoxP3⁺ CD4⁺ T cells from WT and T138- $\beta\beta$ mice (Fig. 6J). Clearly, this poised state in FoxP3⁺ CD4⁺ T cells was only evident in mice carrying the nTreg TCR $\alpha\beta$ -pair, and was not because of an increase in recent thymic emigrants (22). Given this strong bias in differentiation away from Th1 and toward Treg cells and their expression of an nTreg-derived TCR, we consider this T-cell subset as peripheral precursors of nTreg cells, and hence refer to these cells as pre-nTreg cells and not conventional CD4⁺ T cells (Fig. 8). This model is further supported by our data demonstrating that FoxP3⁺ CD4⁺ T cells expressing the nTreg-derived TCR β -chain alone had no bias in their plasticity (Fig. 4). However, the uniqueness of the nTreg-derived TCR β -chain was further supported by their ability to reduce the ability of CD8⁺ T cells to differentiate into FoxP3-expressing CD8⁺ T cells, whereas having no impact on the differentiation into IFN- γ -expressing CD8⁺ T cells (Fig. 4C and Fig. S44). This finding indicated that FoxP3-inducible CD8⁺ T cells might possess TCRs different from the conventional CD8⁺ T-cell pool. The existence of FoxP3⁺ CD4⁺ pre-nTreg cells could also explain why studies that focused on the comparison of TCRs in the pool of conventional T cells and Treg cells found a certain degree of overlap (13–15). In light of our data, we interpret these results not as an overlap of TCRs in conventional T cells and Treg cells, but as existence of pre-nTreg cells within the conventional T-cell population and an overlap of TCRs between pre-nTreg and nTreg cells.

Although the CpG-methylation analysis of Treg-signature genes confirmed that our SCNT-derived model indeed resembled nTreg cells (Fig. 6), it did not explain the poised pre-nTreg phenotype. Thus, future studies on the epigenetic differences in nTreg and pre-nTreg cells, such as DNA methylation of additional loci, histone modifications, and microRNAs are needed to provide new insights into the poised nature of pre-nTreg cells. Given that most experiments use polyclonal CD4⁺ T cells to differentiate T cells into Treg cells and other T-cell subpopulations, most of these experiments might start with a mix of pre-nTreg and so-called Tconv cells and resulting Treg cells might resemble a mix of FoxP3-induced Treg cells. This would be in analogy to the CD8⁺ T-cell compartment, which had been shown to be more complex than previously appreciated (40, 41). In light of the data presented here, we hypothesize that other T-cell subsets might exist within the plenitude of Tconv cell population with a bias in their differentiation capacity toward any T-cell lineage.

Given the very unique situation that pre-nTreg and nTreg cells express the exact same TCR, we performed transcriptome analyses to better understand their differences. We used polyclonal FoxP3⁺ and FoxP3⁺ CD4⁺ T cells for comparison. As shown in Fig. 7, we were able to identify several genes that were differentially expressed among those populations. However, given that the polyclonal FoxP3⁺ CD4⁺ T-cell population might contain a mix of pre-nTreg and Tconv cells, and that the FoxP3⁺ CD4⁺ T-cell population might contain a mix of nTreg and peripherally derived Treg (pTreg) cells, the obtained results must be evaluated critically. A comparison between monoclonal pre-nTreg and nTreg cells revealed unique transcriptional signatures and transcription networks that might provide new insights into the function of nTreg cells. However, more mouse models are needed to identify unique signatures, transcription factors, and surface molecules to unmistakably identify these novel T-cell subpopulations.

Our SCNT nTreg model presented here is in stark contrast to the previously published transgenic Treg models (16–18). Of note, two of these transgenic Treg models were generated using a previously isolated TCR β -chain, such as TRBV6-D1-J2.2 from a CD4⁺ transgenic model recognizing the huCLIP_{81–104} peptide (16). In addition, the FoxP3⁺ CD4⁺ T-cell population in these

Treg transgenic models did not up-regulate FoxP3 upon transfer into lymphopenic hosts (16, 17). Strikingly, our nTreg model demonstrated a well-defined thymic FoxP3⁺ CD4⁺ T-cell population, a TCR β -chain that did impact T-cell development, plasticity, and TCR strength, and the existence of a poised pre-nTreg subset. The observed differences could be because of the approach used (transgenic vs. SCNT), the background of mice (B6 vs. NOD), or could represent different flavors of nTreg cells. However, given the unique features of our nTreg-derived TCR β -chain, an alternative hypothesis that has not been considered so far is that the previously published Treg models might represent pTreg cells. This hypothesis is supported by the observation that the biggest FoxP3⁺ population found in one of the transgenic Treg models can be found in the prostate and its draining lymph node (18).

Taking these data together, we demonstrated herein that our SCNT-derived nTreg model provided new insights into nTreg cell biology. Our data are based on the characterization of a single nTreg model, and more Treg models are needed to determine the characteristics that are, for example, shared by all nTreg cells. One interesting question, in our opinion, is whether there are any nTreg cells that can exist entirely in a FoxP3⁺ state. We were able to identify a new role for TCR β -chain, which offered an explanation for previously reported TCR-dependent and -independent mechanisms of nTreg cell development. In addition, we identified a previously unknown pre-nTreg subset, which is capable of differentiating into FoxP3-expressing cells at high efficiency while almost losing its property to differentiate into Th1 cells. It remains to be determined whether pre-nTreg or nTreg cells can infiltrate inflamed organs more efficiently, and can execute regulatory functions better. The existence of such pre-nTreg cells provides novel therapeutic opportunities, in which drugs that, for example, specifically activate pre-nTreg cells might facilitate the establishment of a suppressive environment, possibly in an organ-specific manner. Consequently, novel and more Treg models are needed to better understand the molecular and functional differences between pre-nTreg, nTreg, and pTreg cells.

Materials and Methods

Mice and Nuclear Transfer. All mice experiments were approved by the Institutional Animal Care and Use Committee at the Scripps Research Institute. Details are given in *SI Materials and Methods*.

TCR Identification. TCR was identified as previously described (19). Briefly, RNA was isolated from splenocytes of SCNT mice (Macherey Nagel), and reverse-transcribed into cDNA (Bio-Rad). PCR was performed using sets of degenerate primers or 5'-RACE. Results were analyzed using the Ensembl Genome Browser (ensembl.org) and the international ImMunoGeneTics information system (www.imgt.org).

Flow Cytometric Analysis and Cell Sorting. Single-cell suspensions of thymus, spleen, or mesenteric lymph node were prepared and red blood cells were lysed. Cells were incubated with various combinations of the following antibodies: CD3, CD4, CD8, CD19, CD25, CD44, CD62L, CD69, CD90.1, Foxp3, $\gamma\delta$ -TCR, NK1.1, and V β 12 (eBioscience and Tonbo). Samples were collected using FACS LSRII (BD) or sorted using FACSAria (BD), and data were analyzed with FlowJo software (Tree Star). Differences between groups were analyzed using two-tailed *t* test (Graphpad Prism software).

T-Cell Differentiation. Details on T-cell differentiation are given in *SI Materials and Methods*.

FoxP3 Stability After in Vitro Differentiation. Foxp3^{GFP}- CD4⁺ T cells were sorted from the spleen of the indicated mice using flow cytometry. For Treg differentiation, 1×10^5 T cells were stimulated with IL-2 (100 U/mL), TGF- β (5 ng/mL; Tonbo), anti-IFN- γ (10 μ g/mL; Tonbo), and Dynabeads Mouse T-Activator CD3/CD28. Four days later, Foxp3^{GFP}-expressing T cells were sorted using flow cytometry and placed back in culture with IL-2 (100 U/mL), anti-IFN- γ (10 μ g/mL; Tonbo), and Dynabeads Mouse T-Activator CD3/CD28. FoxP3 staining was performed by FoxP3/transcription factor staining kit (Tonbo).

Nur77 Assay. CD4⁺ T cells were sorted from the spleen of NOD, T138- $\beta\beta$, or T138-Rag^{-/-} mice and activated with Dynabeads Mouse T-Activator CD3/CD28 in the presence of IL-2. Cells were harvested 5 h after activation and endogenous Nur77 levels were determined using flow cytometry (eBioscience).

Competitive Bone Marrow Transfer. Bone marrow was enriched for progenitor and stem cell population using magnetic separation (Stemcell Technologies). A total of 1×10^5 purified bone marrow cells from NOD-CD90.1 and T138-Rag^{-/-} (CD90.2) mice were mixed at indicated ratios and injected intravenously into irradiated NOD (CD90.1⁺ CD90.2⁺) host mice. Recipient mice were analyzed 7 wk after adoptive transfer.

CpG-Methylation Analysis. All experiments were carried out using male mice. Genomic DNA from indicated cells was extracted using Nucleospin DNA isolation kit according to manufacturer's protocol (Macherey-Nagel). DNA

was then bisulfite treated using Methylcode Bisulfite Conversion kit (Life Technologies). Gene-specific primers were used to amplify genomic regions of interest, as published elsewhere (32). Sequencing data were analyzed using the QUMA (quantification tool for methylation analysis) web-based platform (42).

RNA-Seq and Data Analysis. Details on RNA-preparation, processing, and generation of RNA-Seq libraries, as well as data analysis, are given in *SI Materials and Methods*.

ACKNOWLEDGMENTS. We thank David Nemazee, Changchun Xiao, and Dwight Kono for fruitful discussions, and critical reading of the manuscript; Eugene Ke for support with data analysis; and the flow cytometry core and the department of animal resources at the Scripps Research Institute for outstanding services.

- Sakaguchi S, Sakaguchi N, Asano M, Itoh M, Toda M (1995) Immunologic self-tolerance maintained by activated T cells expressing IL-2 receptor α -chains (CD25). Breakdown of a single mechanism of self-tolerance causes various autoimmune diseases. *J Immunol* 155(3):1151–1164.
- Sakaguchi S, Yamaguchi T, Nomura T, Ono M (2008) Regulatory T cells and immune tolerance. *Cell* 133(5):775–787.
- Hori S, Nomura T, Sakaguchi S (2003) Control of regulatory T cell development by the transcription factor Foxp3. *Science* 299(5609):1057–1061.
- Josefowicz SZ, Lu LF, Rudensky AY (2012) Regulatory T cells: Mechanisms of differentiation and function. *Annu Rev Immunol* 30:531–564.
- Fontenot JD, Gavin MA, Rudensky AY (2003) Foxp3 programs the development and function of CD4⁺CD25⁺ regulatory T cells. *Nat Immunol* 4(4):330–336.
- Khattry R, Cox T, Yasayko SA, Ramsdell F (2003) An essential role for Scurfin in CD4⁺CD25⁺ T regulatory cells. *Nat Immunol* 4(4):337–342.
- Itoh M, et al. (1999) Thymus and autoimmunity: Production of CD25⁺CD4⁺ naturally anergic and suppressive T cells as a key function of the thymus in maintaining immunologic self-tolerance. *J Immunol* 162(9):5317–5326.
- Apostolou I, Sarukhan A, Klein L, von Boehmer H (2002) Origin of regulatory T cells with known specificity for antigen. *Nat Immunol* 3(8):756–763.
- Jordan MS, et al. (2001) Thymic selection of CD4⁺CD25⁺ regulatory T cells induced by an agonist self-peptide. *Nat Immunol* 2(4):301–306.
- Knoechel B, Lohr J, Kahn E, Bluestone JA, Abbas AK (2005) Sequential development of interleukin 2-dependent effector and regulatory T cells in response to endogenous systemic antigen. *J Exp Med* 202(10):1375–1386.
- Pennington DJ, et al. (2006) Early events in the thymus affect the balance of effector and regulatory T cells. *Nature* 444(7122):1073–1077.
- Bosco N, Agnes F, Rolink AG, Ceredig R (2006) Peripheral T cell lymphopenia and concomitant enrichment in naturally arising regulatory T cells: The case of the pre-Talpa gene-deleted mouse. *J Immunol* 177(8):5014–5023.
- Hsieh CS, Zheng Y, Liang Y, Fontenot JD, Rudensky AY (2006) An intersection between the self-reactive regulatory and nonregulatory T cell receptor repertoires. *Nat Immunol* 7(4):401–410.
- Pacholczyk R, et al. (2007) Nonself-antigens are the cognate specificities of Foxp3⁺ regulatory T cells. *Immunity* 27(3):493–504.
- Wong J, et al. (2007) Adaptation of TCR repertoires to self-peptides in regulatory and nonregulatory CD4⁺ T cells. *J Immunol* 178(11):7032–7041.
- Bautista JL, et al. (2009) Intracolon competition limits the fate determination of regulatory T cells in the thymus. *Nat Immunol* 10(6):610–617.
- Leung MW, Shen S, Lafaille JJ (2009) TCR-dependent differentiation of thymic Foxp3⁺ cells is limited to small clonal sizes. *J Exp Med* 206(10):2121–2130.
- Malchow S, et al. (2013) Aire-dependent thymic development of tumor-associated regulatory T cells. *Science* 339(6124):1219–1224.
- Kirak O, et al. (2010) Transnuclear mice with pre-defined T cell receptor specificities against *Toxoplasma gondii* obtained via SCNT. *J Vis Exp* (43):2168.
- Kirak O, et al. (2010) Transnuclear mice with predefined T cell receptor specificities against *Toxoplasma gondii* obtained via SCNT. *Science* 328(5975):243–248.
- Hsieh CS, Lee HM, Lio CW (2012) Selection of regulatory T cells in the thymus. *Nat Rev Immunol* 12(3):157–167.
- Paiva RS, et al. (2013) Recent thymic emigrants are the preferential precursors of regulatory T cells differentiated in the periphery. *Proc Natl Acad Sci USA* 110(16):6494–6499.
- Cozzo Picca C, et al. (2011) CD4⁺CD25⁺Foxp3⁺ regulatory T cell formation requires more specific recognition of a self-peptide than thymocyte deletion. *Proc Natl Acad Sci USA* 108(36):14890–14895.
- Feuerer M, et al. (2007) Enhanced thymic selection of FoxP3⁺ regulatory T cells in the NOD mouse model of autoimmune diabetes. *Proc Natl Acad Sci USA* 104(46):18181–18186.
- Hinterberger M, et al. (2010) Autonomous role of medullary thymic epithelial cells in central CD4⁺ T cell tolerance. *Nat Immunol* 11(6):512–519.
- Moran AE, et al. (2011) T cell receptor signal strength in Treg and iNKT cell development demonstrated by a novel fluorescent reporter mouse. *J Exp Med* 208(6):1279–1289.
- Azzam HS, et al. (1998) CD5 expression is developmentally regulated by T cell receptor (TCR) signals and TCR avidity. *J Exp Med* 188(12):2301–2311.
- Azzam HS, et al. (2001) Fine tuning of TCR signaling by CD5. *J Immunol* 166(9):5464–5472.
- Kim HP, Leonard WJ (2007) CREB/ATF-dependent T cell receptor-induced Foxp3 gene expression: A role for DNA methylation. DNA methylation controls Foxp3 gene expression. *J Exp Med* 204(7):1543–1551.
- Zheng Y, et al. (2010) Role of conserved non-coding DNA elements in the Foxp3 gene in regulatory T-cell fate. *Nature* 463(7282):808–812.
- Polansky JK, et al. (2008) DNA methylation controls Foxp3 gene expression. *Eur J Immunol* 38(6):1654–1663.
- Ohkura N, et al. (2012) T cell receptor stimulation-induced epigenetic changes and Foxp3 expression are independent and complementary events required for Treg cell development. *Immunity* 37(5):785–799.
- Deaglio S, et al. (2007) Adenosine generation catalyzed by CD39 and CD73 expressed on regulatory T cells mediates immune suppression. *J Exp Med* 204(6):1257–1265.
- Pan F, et al. (2009) Eos mediates Foxp3-dependent gene silencing in CD4⁺ regulatory T cells. *Science* 325(5944):1142–1146.
- Thornton AM, et al. (2010) Expression of Helios, an Ikaros transcription factor family member, differentiates thymic-derived from peripherally induced Foxp3⁺ T regulatory cells. *J Immunol* 184(7):3433–3441.
- Shin DS, et al. (2014) Regulatory T cells suppress CD4⁺ T cells through NFAT-dependent transcriptional mechanisms. *EMBO Rep* 15(9):991–999.
- Vaeth M, et al. (2012) Dependence on nuclear factor of activated T-cells (NFAT) levels discriminates conventional T cells from Foxp3⁺ regulatory T cells. *Proc Natl Acad Sci USA* 109(40):16258–16263.
- Wu Y, et al. (2006) FOXP3 controls regulatory T cell function through cooperation with NFAT. *Cell* 126(2):375–152.
- Singh Y, Ferreira C, Chan AC, Dyson J, Garden OA (2010) Restricted TCR- α CDR3 diversity disadvantages natural regulatory T cell development in the B6.2.16 beta-chain transgenic mouse. *J Immunol* 185(6):3408–3416.
- Newell EW, Sigal N, Bendall SC, Nolan GP, Davis MM (2012) Cytometry by time-of-flight shows combinatorial cytokine expression and virus-specific cell niches within a continuum of CD8⁺ T cell phenotypes. *Immunity* 36(1):142–152.
- Newell EW, et al. (2013) Combinatorial tetramer staining and mass cytometry analysis facilitate T-cell epitope mapping and characterization. *Nat Biotechnol* 31(7):623–629.
- Kumaki Y, Oda M, Okano M (2008) QUMA: Quantification tool for methylation analysis. *Nucleic Acids Res* 36(Web Server issue):W170–W175.
- Dobin A, et al. (2013) STAR: Ultrafast universal RNA-seq aligner. *Bioinformatics* 29(1):15–21.
- Heinz S, et al. (2010) Simple combinations of lineage-determining transcription factors prime cis-regulatory elements required for macrophage and B cell identities. *Mol Cell* 38(4):576–589.
- Robinson MD, McCarthy DJ, Smyth GK (2010) edgeR: A Bioconductor package for differential expression analysis of digital gene expression data. *Bioinformatics* 26(1):139–140.
- de Hoon MJ, Imoto S, Nolan J, Miyano S (2004) Open source clustering software. *Bioinformatics* 20(9):1453–1454.
- Saldanha AJ (2004) Java Treeview—Extensible visualization of microarray data. *Bioinformatics* 20(17):3246–3248.
- Wang J, Duncan D, Shi Z, Zhang B (2013) WEB-based GENE SeT Analysis Toolkit (WebGestalt): Update 2013. *Nucleic Acids Res* 41(Web Server issue):W77–W83.
- Zhang B, Kirov S, Snoddy J (2005) WebGestalt: An integrated system for exploring gene sets in various biological contexts. *Nucleic Acids Res* 33(Web Server issue):W741–W748.